

## Muon-electron scattering at NNLO with McMULE

---

**Marco Rocco**<sup>a,\*</sup>

<sup>a</sup>*Paul Scherrer Institut  
CH-5232 Villigen PSI, Switzerland*

*E-mail:* [marco.rocco@psi.ch](mailto:marco.rocco@psi.ch)

A recently proposed experiment, MUonE, aims to extract the hadronic vacuum polarisation contribution to the muon  $g - 2$  from muon-electron scattering at low energy. The extrapolation requires that both experimental and theoretical uncertainties do not exceed 10 ppm. This corresponds, at least, to next-to-next-to-leading-order (NNLO) QED corrections to  $e\mu \rightarrow e\mu$ . I will discuss the implementation of a Monte Carlo integrator for this process in the McMULE framework [1], which provides infrared-safe differential results at said order in QED. An approximation of the MUonE setup provides some phenomenological results and sheds light on the need for beyond-NNLO corrections, which are currently under study within McMULE.

*16th International Symposium on Radiative Corrections:  
Applications of Quantum Field Theory to Phenomenology (RADCOR2023)  
28th May - 2nd June, 2023  
Crieff, Scotland, UK*

---

\*Speaker

## 1. Introduction

Excluding new physics, the hadronic vacuum polarisation (HVP) contribution to the muon anomalous magnetic moment,  $a_\mu = (g - 2)/2$ , is generally referred to as the source of the long-standing discrepancy between experimental measurements [2–4] and Standard Model (SM) predictions. Currently, there is not an agreement among the latter, as predictions using lattice QCD differ from those employing data-driven dispersive calculations. In contrast to dispersive predictions [5], whose discrepancy with the experiment amounts up to  $5\sigma$ , a recent calculation in lattice QCD [6] drastically reduces the discrepancy. In this scenario, a different approach to a data-driven calculation, expressed e.g. by the MUonE experiment [7, 8], is decisive to further disentangle the problem.

Traditional dispersive calculations rely on experimental inputs from  $e^+e^- \rightarrow \text{hadrons}$ , measured in the time-like region ( $s > 0$ ) at energies around 1-10 GeV, where numerous hadronic resonances hamper the experimental precision.

On the other hand, the MUonE experiment consists of a 160 GeV muon beam colliding on a fixed target of atomic electrons, in a pure  $t$ -channel. From the measurement of the scattering angles of muons and electrons,  $\theta_\mu$  and  $\theta_e$ , in elastic events, the HVP contribution to the running of the electromagnetic coupling,  $\alpha(t(x) < 0)$ , can be reconstructed via a template fit in the space-like region, where no resonance hampers the measurement. The formula [8]

$$a_\mu^{\text{HVP}} = \frac{\alpha}{\pi} \int_0^1 dx (1-x) \Delta\alpha^{\text{had}}(t(x)), \quad t(x) = -\frac{x^2 m_\mu^2}{1-x}, \quad (1)$$

yields the HVP contribution to the muon anomaly. Figure 1 shows a simulation of the running of  $\alpha$ , split into a leptonic and a hadronic part. The former is computed perturbatively, while the second employs the library `alphaQED` [9].

The kinematics of MUonE is particularly favourable, as the area accessible to the experiment covers most of the HVP contribution in Figure 1, i.e. corresponding to higher values of  $x$ , or equivalently smaller values of  $\theta_e$ . Further, this allows to define a normalisation region, where the HVP signal is much lower.

However, the accuracy of the total experimental and theoretical error should not exceed 10 ppm, as the signal of the experiment is  $\mathcal{O}(10^{-3})$ , and the HVP needs to be extracted with a precision below one percent, in order to match the statistical error of the other evaluations.

On the theoretical side, there has been a coordinated effort [10] aiming at developing two completely independent Monte Carlo event generators for muon-electron scattering. At least an NNLO calculation in QED is mandatory to reach the precision required, and the results at this order suggest the need for the resummation of large logarithms and the calculation of (the dominant part of) the N<sup>3</sup>LO corrections. In addition to higher-order QED effects, nuclear effects as well as pion and lepton-pair production have to be taken into account [11], but will not be considered in this contribution.

The MESMER Monte Carlo provides the complete set of electroweak NLO corrections [12], as well as QED NNLO corrections [13, 14], using an approximation for genuine two-loop four-point topologies. In order to cope with infrared divergences photon-mass regularisation combined with a slicing approach is employed. In parallel, the McMULE framework [15] offers another

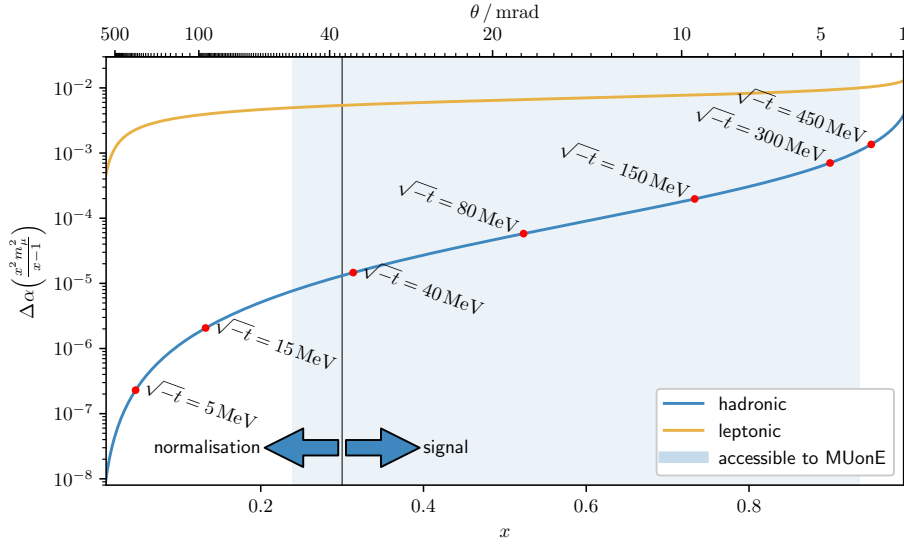


**Figure 1:** HVP contribution to the running of  $\alpha$  for space-like kinematics, computed as the NLO correction to muon-electron scattering due to HVP insertions, as a function of  $x$  and  $\theta_e$ . The contribution due to leptonic VP insertions is also given for comparison, along with the kinematic region accessible to MUonE.

efficient environment to reach the desired level of accuracy. Section 2 discusses the implementation in McMULE of muon-electron scattering at NNLO in QED, which can serve as a Monte Carlo generator (at present, integrator) for the MUonE experiment. A subset of the results is presented in Section 3, before concluding in Section 4.

## 2. McMULE for MUonE

The implementation of muon-electron scattering at NNLO in the McMULE framework, along with results and discussion, is presented in greater detail in [1] and [16]. Here follows a summary, with a particular focus on phenomenology.

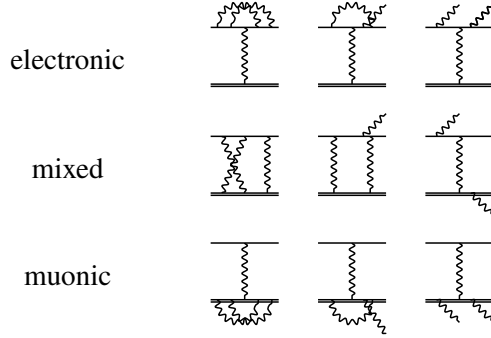
The general idea behind McMULE is the adaptation of techniques developed and employed in the context of higher-order perturbative QCD, to higher-order studies in QED. For example, McMULE uses dimensional regularisation and a generalisation of the FKS method [17, 18] to any order in the electromagnetic coupling,  $\text{FKS}^\ell$  [19], for the subtraction of soft divergences. In fact, MUonE observables are not collinear safe, and therefore strongly depend on fermion-mass effects. Thus, for fully differential predictions, taking those into account is strictly necessary. At the same time, lepton masses regulate collinear divergences, leaving soft divergences only.

Further, the same machinery developed to handle one- and multi-loop integrals can be adapted to QED, where the presence of additional scales, such as the lepton masses, makes loop integrations more difficult. For one-loop problems, McMULE employs OPENLOOPS [20, 21], which proved to be remarkably stable except for phase-space regions where a photon is particularly soft, or a pseudo-collinear configuration leads to the presence of large logarithms. A good numerical stability is recovered using next-to-soft (NTS) stabilisation [22, 23] for such regions, i.e. employing the leading- and next-to-leading-soft terms in the photon-energy expansion of the relevant matrix

element, instead of the full matrix element. With two-loop diagrams no automatic procedure is able to deal with generic processes. It is then necessary to resort to external results that consider the particular process of interest. These results are often built for QCD, where the mass of the light quarks can be neglected. Thus, McMULE employs calculations where the mass of the fermion is neglected, but can recover those neglected effects via massification [24–26].

A more detailed discussion about the methods used in McMULE (and a validation of them) can be found in the original muon-electron scattering paper [1], or elsewhere in these proceedings [27]. For the purpose of the present contribution, it is sufficient to say that muon-electron scattering at NNLO is implemented as follows. Contributions at NLO (real and virtual) and NNLO (double-real, real-virtual and double-virtual) are divided into photonic and fermionic. The latter are those containing a fermionic vacuum polarisation insertion, and were calculated using the hyperspherical method [28], then validated by a second calculation done via a dispersive method [29].

In general, both photonic and fermionic contributions can be subdivided into three gauge-invariant subsets according to their formal leptonic charge. As for the sample diagrams below, contributions where photon radiation only attaches to the electron (muon) line are called electronic (muonic), all other contributions are referred to as mixed. In the McMULE framework, each contribution can be computed separately, allowing the user to study the impact of different classes and to infer possible hierarchies among them.



Double-virtual electronic and muonic contributions were computed with full mass dependence, using the analytic expressions for the heavy quark form factors of [30], while mixed double-virtual contributions, which involve genuine two-loop four-point topologies, were computed applying massification to the results of [31, 32], which employ the master integrals computed in [32–34]. This is the only approximation made in the McMULE prediction, amounting to the neglect, at NNLO, of terms that are polynomially suppressed in the electron-mass expansion of the double-virtual contribution. NTS stabilisation was then applied to all real-virtual contributions, in order to achieve the desired numerical stability. As shown in the original paper, the use of NTS expansions results in the neglect of terms that are much below the 10 ppm requirement by MUonE.

A number of internal and external tests were carried out in order to validate the results, cf. Section 4 of [1]. Here we comment on the comparison of the mixed contributions to the photonic NNLO correction, which have been calculated both in MESMER and in McMULE. Since the two frameworks employ different scheme to handle IR divergences, a comparison between the two results represents a completely independent check. As the calculation in [14] is complete up to the mixed two-loop contribution, it is possible to compare the mixed NLO correction to  $\mu e \rightarrow \mu e \gamma$ ,

which is physical and corresponds to the double-real and real-virtual contributions to muon-electron scattering. In order to check the numerical stability of the real-virtual implementation, small photon energy cuts of  $\{10^{-6}, 10^{-5}, 10^{-4}\} \times \sqrt{s}/2$  were used. Perfect agreement was found between the two codes for the total cross section as well as for differential distributions, as shown in Figure 2, at sub-percent level.

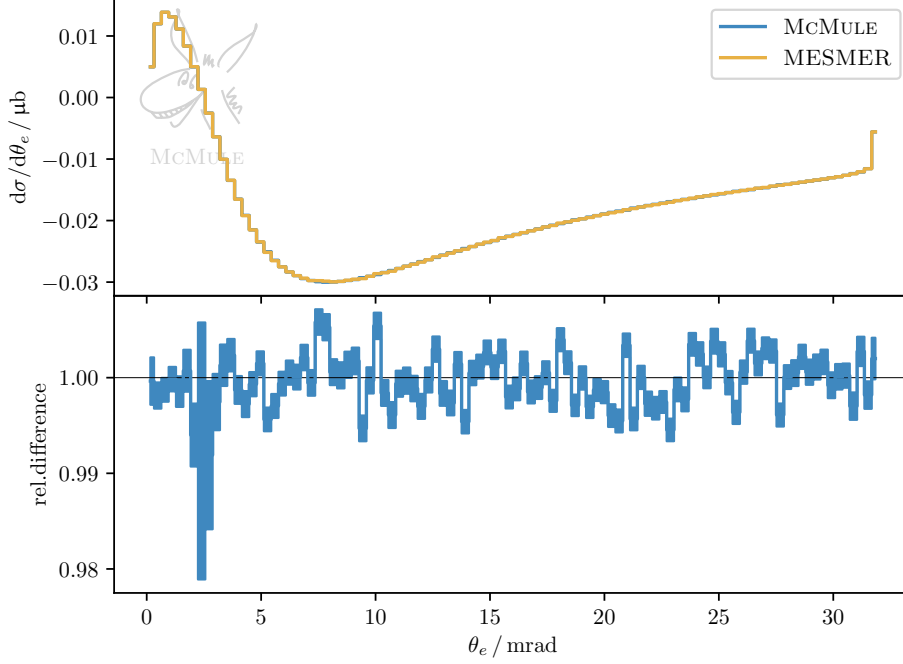


**Figure 2:** Top: NNLO double-real and real-virtual contributions to muon-electron scattering as differential distributions w.r.t.  $\theta_e$ , computed by MESMER (yellow) and McMULE (blue). A small photon energy cut of  $10^{-6} \times \sqrt{s}/2$  was used. Bottom: Ratio between the two predictions. The larger oscillation is unphysical, corresponding to the zero crossing of the distributions.

### 3. Results

This section presents some results for muon-electron scattering at NNLO, with the characteristics of the MUonE experiment in mind. The kinematics is defined by

$$e^-(p_1) \mu^\pm(p_2) \rightarrow e^-(p_3, E_e, \theta_e) \mu^\pm(p_4, E_\mu, \theta_\mu) + \{\gamma(k_1) \gamma(k_2)\}, \quad (2)$$

with the outgoing electron and muon energy,  $E_e$  and  $E_\mu$ , and the electron and muon scattering angle with respect to the beam axis,  $\theta_e$  and  $\theta_\mu$ . The muon beam energy is set to 160 GeV, consistent with the M2 beam line at CERN North Area [35]. A cut is imposed on the energy of the outgoing electron,  $E_e > 1$  GeV, which is equivalent to a cut on the minimal value of  $|t|$ , in order to cure the singular behaviour of  $d\sigma/dt \sim t^{-2}$ , where  $t$  is the usual Mandelstam invariant. A cut on  $\theta_\mu$  can be

used to remove most of the background. Hence, for the results shown here,  $\theta_\mu > 0.3$  mrad was also required.

Given this kinematical setup, McMULE is able to produce differential distributions for any infrared-safe observable. At present, it does not generate events and can only act as a Monte Carlo integrator. However, the possibility to generate events will be available in the near future [36].

In this contribution, the focus is on differential distributions w.r.t. the scattering angle of the electron, as this is the main interest of the MUonE experiment, in particular for a beam of negative muons. The whole set of results is instead presented in the original paper and publicly available at the McMULE Zenodo repository [37].

Figure 3 and 4 show, in the upper panel, the LO and (N)NLO angular distributions, and, in the lower panel, the  $K$  factor for the NLO and NNLO distributions, defined as

$$K^{(i)} - 1 = \frac{\sigma_i}{\sigma_{i-1}}, \quad (3)$$

where  $\sigma_k = \sum_{i=0}^k \sigma^{(i)}$  is given by the sum of the order-by-order contributions,  $\sigma^{(i)}$ , to the  $N^k$ LO integrated cross section. In addition, the  $K$  factor of the signal is also shown, corresponding to the hadronic part of the NLO fermionic contribution.

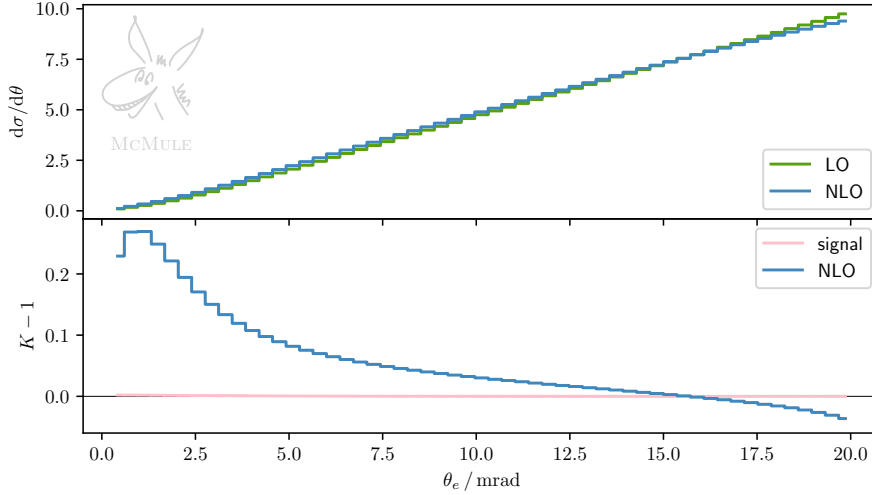


**Figure 3:** Top: LO (green) and NLO (blue) differential cross section w.r.t.  $\theta_e$ . Bottom:  $K$  factors of the NLO correction and the signal of the MUonE experiment (pink), i.e. the NLO HVP contribution.

(N)NLO corrections amount up to 20% (0.2%), particularly for small electron scattering angles, or equivalently for large electron energies, where photon emission is forced to be soft. In this kinematical configuration, the signal is completely outweighed by the NLO correction, and turns out to be of the same order or smaller than the NNLO correction. Further, the enhancement observed in the small- $\theta_e$  region suggests the need for a more reliable description of the region where large logarithms cause such behaviour.

In order to achieve a well-defined extraction of the signal, not hampered by such dominant QED corrections in the background, a possible way to proceed is to discriminate elastic scattering events

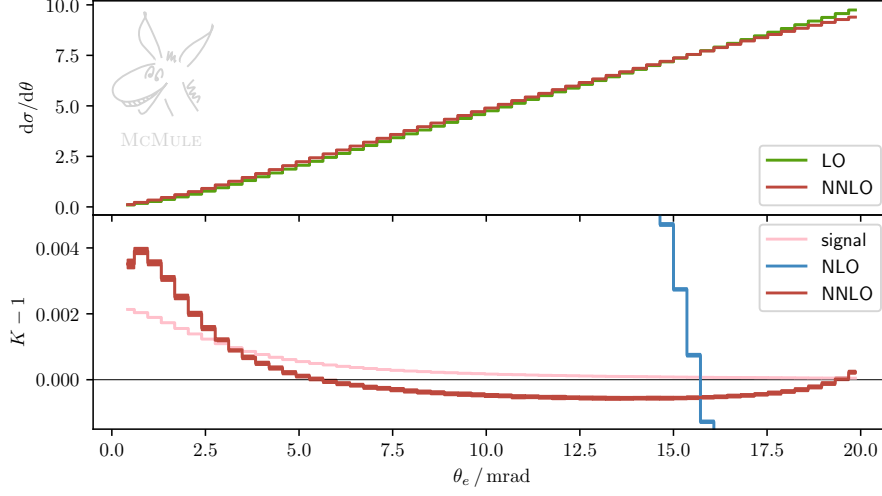


**Figure 4:** Top: LO (green) and NNLO (red) differential cross section w.r.t.  $\theta_e$ . Bottom:  $K$  factors of the NLO and NNLO correction, and the signal of the MUonE experiment (pink), i.e. the NLO HVP contribution.

from the otherwise kinematically allowed radiative events and processes. This can be obtained in terms of the elasticity constraint that relates muon and electron scattering angles in the absence of photons, shown in Figure 5. For example, the requirement  $0.9 < \theta_\mu / \theta_\mu^{\text{el}} < 1.1$ , where  $\theta_\mu^{\text{el}}$  is the

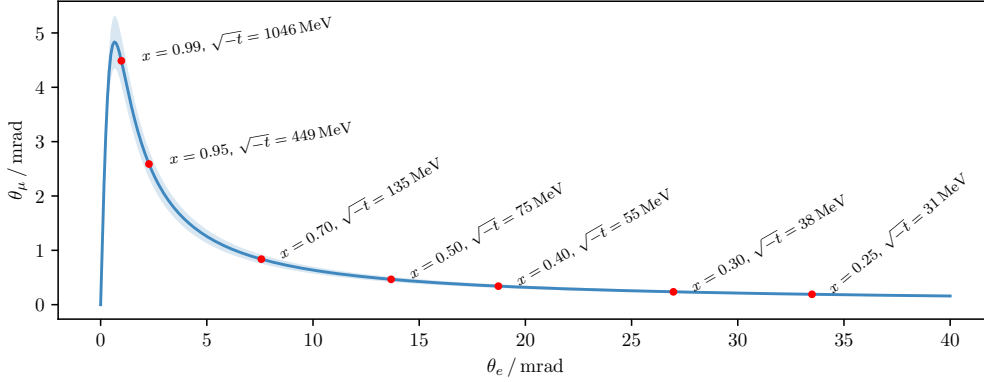


**Figure 5:**  $\theta_\mu$  as a function of  $\theta_e$  for elastic events. The light-blue band corresponds to the elasticity cut.

muon scattering angle as defined in Figure 5 as a function of the electron scattering angle, can act as a veto for hard radiation. The angular distributions in the presence of this additional elasticity cut are displayed in Figure 6.

As expected from an evenly-distributed soft enhancement, the  $K$  factor is significantly reduced and flattened. In this context, the NLO correction can be subtracted more efficiently, and the signal can be extracted on top of the NNLO correction, which is now, in general, smaller. However, such a kinematical constraint is not ideal from the experimental perspective. It would cut off many events, yielding issues in terms of statistics, and would also complicate the estimate of systematic uncertainties, as it would lead to a complex practical implementation. At present, the alternative

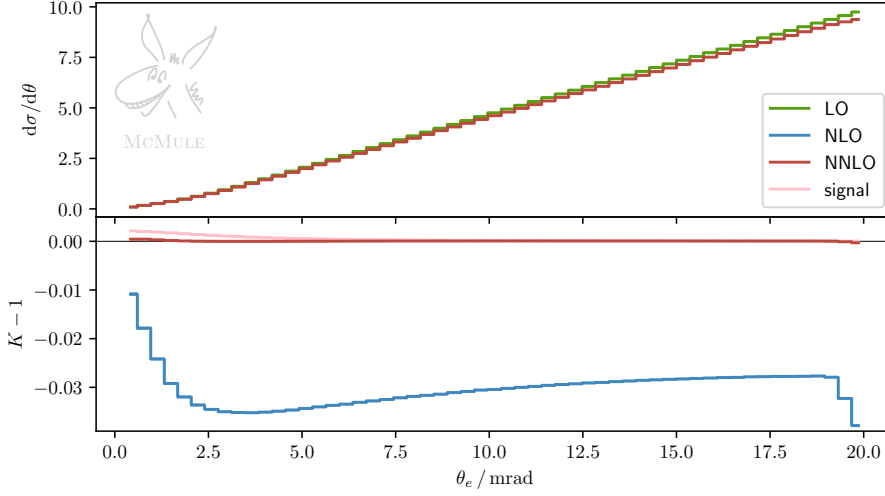


**Figure 6:** Top: LO (green) and NNLO (red) differential cross section w.r.t.  $\theta_e$ . Bottom:  $K$  factors of the NLO and NNLO correction, and the signal of the MUonE experiment (pink), i.e. the NLO HVP contribution. All curves are obtained after applying the elasticity cut discussed in the text.

proposed by the experiment is to employ a template fit to extract the HVP, as discussed in [38]. Nonetheless, a study with the elasticity cut is still of theoretical interest.

#### 4. Conclusions and outlook

We have reviewed the implementation in the McMULE framework of muon-electron scattering at NNLO in QED, as well as some of the results presented therein. This corresponds to the first result at NNLO for a two-to-two process in QED with two different non-vanishing masses on the external lines. A more detailed description of the methods employed can be found elsewhere in these proceedings [27].

The MUonE experiment may benefit from these results for the extraction of the HVP contribution to the muon  $g - 2$ . The McMULE effort is part of a bigger theoretical effort [10], whose aim is to provide the most precise prediction for muon-electron scattering, in order to match the 10 ppm precision goal. The magnitude of the NNLO corrections at differential level, around  $10^{-3}$ , is still too large compared to said goal. Thus, higher-order predictions beyond NNLO can certainly help in that direction. Furthermore, it is mandatory to make an effort towards a more reliable description of the region where radiation leads to an enhancement through large logarithms.

An  $N^3$ LO prediction (or at least the dominant part of it) and a more precise description of large-log regions, through resummation or via the implementation of a parton shower, are on the agenda of an ongoing effort, started with a series of workstops in 2022 and 2023 [39, 40].

**Acknowledgement** I acknowledge support from the Swiss National Science Foundation (SNSF) under grant 200020\_20738. A huge thank you to all the colleagues of the original paper [1], upon which this contribution is mainly based.



## References

- [1] A. Broggio et al., *Muon-electron scattering at NNLO*, *JHEP* **01** (2023) 112 [2212.06481].
- [2] MUON G-2 collaboration, G. W. Bennett et al., *Final Report of the Muon E821 Anomalous Magnetic Moment Measurement at BNL*, *Phys. Rev. D* **73** (2006) 072003 [hep-ex/0602035].
- [3] MUON G-2 collaboration, B. Abi et al., *Measurement of the Positive Muon Anomalous Magnetic Moment to 0.46 ppm*, *Phys. Rev. Lett.* **126** (2021) 141801 [2104.03281].
- [4] MUON G-2 collaboration, D. P. Aguillard et al., *Measurement of the Positive Muon Anomalous Magnetic Moment to 0.20 ppm*, 2308.06230.
- [5] T. Aoyama et al., *The anomalous magnetic moment of the muon in the Standard Model*, *Phys. Rept.* **887** (2020) 1 [2006.04822].
- [6] S. Borsanyi et al., *Leading hadronic contribution to the muon magnetic moment from lattice QCD*, *Nature* **593** (2021) 51 [2002.12347].
- [7] G. Abbiendi et al., *Measuring the leading hadronic contribution to the muon g-2 via  $\mu e$  scattering*, *Eur. Phys. J. C* **77** (2017) 139 [1609.08987].
- [8] C. M. Carloni Calame, M. Passera, L. Trentadue and G. Venanzoni, *A new approach to evaluate the leading hadronic corrections to the muon g-2*, *Phys. Lett. B* **746** (2015) 325 [1504.02228].
- [9] F. Jegerlehner. <http://www-com.physik.hu-berlin.de/~fjeger/software.html>.
- [10] P. Banerjee et al., *Theory for muon-electron scattering @ 10 ppm: A report of the MUonE theory initiative*, *Eur. Phys. J. C* **80** (2020) 591 [2004.13663].
- [11] E. Budassi, C. M. Carloni Calame, C. L. Del Pio and F. Piccinini, *Single  $\pi^0$  production in  $\mu e$  scattering at MUonE*, *Phys. Lett. B* **829** (2022) 137138 [2203.01639].
- [12] M. Alacevich, C. M. Carloni Calame, M. Chiesa, G. Montagna, O. Nicrosini and F. Piccinini, *Muon-electron scattering at NLO*, *JHEP* **02** (2019) 155 [1811.06743].
- [13] C. M. Carloni Calame, M. Chiesa, S. M. Hasan, G. Montagna, O. Nicrosini and F. Piccinini, *Towards muon-electron scattering at NNLO*, *JHEP* **11** (2020) 028 [2007.01586].
- [14] E. Budassi, C. M. Carloni Calame, M. Chiesa, C. L. Del Pio, S. M. Hasan, G. Montagna et al., *NNLO virtual and real leptonic corrections to muon-electron scattering*, *JHEP* **11** (2021) 098 [2109.14606].
- [15] McMULE Team. <https://mule-tools.gitlab.io/>.
- [16] T. Engel, *Muon-Electron Scattering at NNLO*, PhD Thesis, Universität Zürich, 9, 2022.

- [17] S. Frixione, Z. Kunszt and A. Signer, *Three jet cross-sections to next-to-leading order*, *Nucl. Phys. B* **467** (1996) 399 [[hep-ph/9512328](#)].
- [18] R. Frederix, S. Frixione, F. Maltoni and T. Stelzer, *Automation of next-to-leading order computations in QCD: The FKS subtraction*, *JHEP* **10** (2009) 003 [[0908.4272](#)].
- [19] T. Engel, A. Signer and Y. Ulrich, *A subtraction scheme for massive QED*, *JHEP* **01** (2020) 085 [[1909.10244](#)].
- [20] F. Buccioni, S. Pozzorini and M. Zoller, *On-the-fly reduction of open loops*, *Eur. Phys. J. C* **78** (2018) 70 [[1710.11452](#)].
- [21] F. Buccioni, J.-N. Lang, J. M. Lindert, P. Maierhöfer, S. Pozzorini, H. Zhang et al., *OpenLoops 2*, *Eur. Phys. J. C* **79** (2019) 866 [[1907.13071](#)].
- [22] P. Banerjee, T. Engel, N. Schalch, A. Signer and Y. Ulrich, *Bhabha scattering at NNLO with next-to-soft stabilisation*, *Phys. Lett. B* **820** (2021) 136547 [[2106.07469](#)].
- [23] T. Engel, A. Signer and Y. Ulrich, *Universal structure of radiative QED amplitudes at one loop*, *JHEP* **04** (2022) 097 [[2112.07570](#)].
- [24] A. A. Penin, *Two-loop photonic corrections to massive Bhabha scattering*, *Nucl. Phys. B* **734** (2006) 185 [[hep-ph/0508127](#)].
- [25] T. Becher and K. Melnikov, *Two-loop QED corrections to Bhabha scattering*, *JHEP* **06** (2007) 084 [[0704.3582](#)].
- [26] T. Engel, C. Gnendiger, A. Signer and Y. Ulrich, *Small-mass effects in heavy-to-light form factors*, *JHEP* **02** (2019) 118 [[1811.06461](#)].
- [27] Y. Ulrich, *QED at NNLO and beyond for precision experiments*, in *16th International Symposium on Radiative Corrections: Applications of Quantum Field Theory to Phenomenology*, 9, 2023.
- [28] M. Fael, *Hadronic corrections to  $\mu$ -e scattering at NNLO with space-like data*, *JHEP* **02** (2019) 027 [[1808.08233](#)].
- [29] M. Fael and M. Passera, *Muon-Electron Scattering at Next-To-Next-To-Leading Order: The Hadronic Corrections*, *Phys. Rev. Lett.* **122** (2019) 192001 [[1901.03106](#)].
- [30] W. Bernreuther, R. Bonciani, T. Gehrmann, R. Heinesch, T. Leineweber, P. Mastrolia et al., *Two-loop QCD corrections to the heavy quark form-factors: The Vector contributions*, *Nucl. Phys. B* **706** (2005) 245 [[hep-ph/0406046](#)].
- [31] R. Bonciani et al., *Two-Loop Four-Fermion Scattering Amplitude in QED*, *Phys. Rev. Lett.* **128** (2022) 022002 [[2106.13179](#)].
- [32] M. K. Mandal, P. Mastrolia, J. Ronca and W. J. Bobadilla Torres, *Two-loop scattering amplitude for heavy-quark pair production through light-quark annihilation in QCD*, *JHEP* **09** (2022) 129 [[2204.03466](#)].

- [33] P. Mastrolia, M. Passera, A. Primo and U. Schubert, *Master integrals for the NNLO virtual corrections to  $\mu e$  scattering in QED: the planar graphs*, *JHEP* **11** (2017) 198 [1709.07435].
- [34] S. Di Vita, S. Laporta, P. Mastrolia, A. Primo and U. Schubert, *Master integrals for the NNLO virtual corrections to  $\mu e$  scattering in QED: the non-planar graphs*, *JHEP* **09** (2018) 016 [1806.08241].
- [35] MUONE collaboration, E. Spedicato, *Status of the MUonE experiment*, *PoS EPS-HEP2021* (2022) 642.
- [36] Y. Ulrich, *Generating events at NNLO with McMULE, in preparation* (2023) .
- [37] McMULE Team, “McMULE dataset.” <https://doi.org/10.5281/zenodo.6541686>.
- [38] G. Abbiendi, *Status of the MUonE experiment*, *Phys. Scripta* **97** (2022) 054007 [2201.13177].
- [39] Y. Ulrich, “N<sup>3</sup>LO kick-off workstop/thinkstart, Durham, 3–5 August, 2022.” <https://conference.ippp.dur.ac.uk/event/1104/>.
- [40] A. Kupsc, A. Signer, Y. Ulrich and G. Venanzoni, “5th Workstop/Thinkstart: Radiative corrections and Monte Carlo tools for Strong 2020, Zürich, 5–9 June, 2023.” <https://indico.psi.ch/event/13707/>.